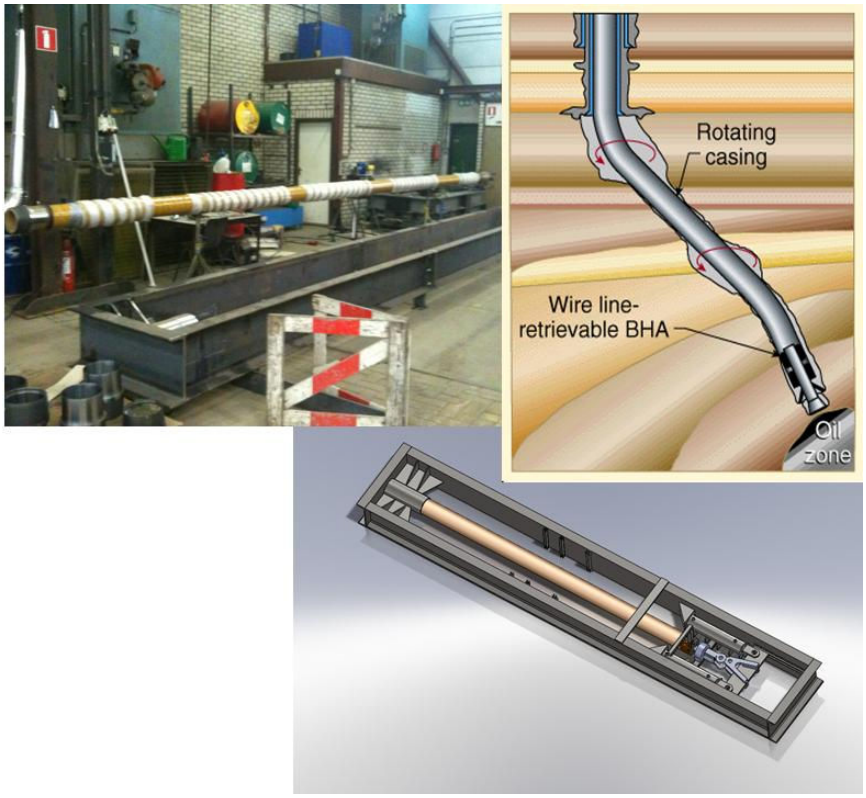
An investigation of the stress-strain behaviour of a GRE cylindrical structure used for a drilling-with-casing application and its influence on torsional vibrations



TU Delft

Department of Geotechnology

Delft University of Technology

Title	:	An investigation of the stress-strain behaviour and hysteresis of a GRE cylindrical structure used for a drilling-with-casing application and its influence on torsional vibrations
Author	:	Jan Willem van der Poll
Date	:	July, 2010
Supervisors	:	Prof. dr. ir. J.D. Jansen, , ir. A. Nagelhout, ir T. Bakker
Exam committee	:	dr. I. Fernandez Villegas, .ing. G.L.J. de Blok, E. Burnaby Lautier
TA Report number	:	AES/PE/10-09
Postal Address	:	Section for Petroleum Engineering Department of Geotechnology Delft University of Technology P.O. Box 5028 The Netherlands
Telephone	:	+31 (0) 15 2781328 (secretary)
Telefax	:	+31 (0) 15 2781189

Copyright ©2010 Section for Petroleum Engineering

All rights reserved.
No parts of this publication may be reproduced,
Stored in a retrieval system, or transmitted,
In any form or by any means, electronic,
Mechanical, photocopying, recording, or otherwise,
Without the prior written permission of the
Section for Petroleum Engineering

Table of Content

TABLE OF FIGURES 5
TABLE OF TABLES 7
ABSTRACT 8
1 THESIS OVERVIEW AND OBJECTIVES 10
2 GENERAL INTRODUCTION 13
2.1 Delft Aardwarmte Project (DAP) 13
2.2 The GRE pipe 15
2.2.1 Stress-strain behaviour 15
2.2.2 Hysteresis 15
2.2.3 The laminate structure 17
3 TORSIONAL VIBRATIONS 18
3.1 Introduction 18
3.2 Self-excited vibrations 19
4 TORQUE AND DRAG (TanD) 22
4.1 Introduction to TanD 22
4.2 TanD results 24
4.2.1 Results of the TanD analysis 24
4.2.2 The $7^5/_8$" section to TD 24
5 STRESS-STRAIN TESTING METHODS 26
5.1 Testing for non-linearity 26
5.2 Testing hysteresis 26
5.3 The testing bench 27
5.3.1 The testing section 29
5.4Calculating the elasticity and shear modulus 35
6 RESULTS 36
6.1 Stress-strain behaviour in axial direction 36
6.2 Result of the tangential stress-strain behaviour 39
6.3 The elongation and twist of the drill string 40
6.4 Tangential stress-strain behaviour combined with axial tension 41
6.5 A comparison between GRE and steel concerning torsional vibrations 44
6.6 Dampening due to hysteresis 46
7 CONCLUSIONS AND RECOMMENDATIONS 46
7.1 Conclusions 46
7.2 Recommendations 48
APPENDICES 51

Appendix A Exact layering of GRE pipe 51
Appendix B Matlab code torsional vibrations 52
Appendix C The well trajectory of the input data and an extension on the equations used for the TanD calculation1 54
REFERENCES 58

Table of figures

Figure 2.1 Schematically this drawing shows the injector and producer doublet 14

Figure 2.2 Typical stress-strain type graph with a hysteresis profile. 16

Figure 2.3 Unidirectional tape on a roll. 17

Figure 3.1 Schematic of the drill string as a torsional pendulum. (Jansen 1993). 20

Figure 4.1 The left figure shows a schematic of the forces in on the hole giving an overall net side load of F_n. The right side shows the force distribution when pulling out of the hole (Johancsik et al. 1984). 23

Figure 4.2 This graph shows the maximum expected forces in the producer well. 25

Figure 4.3 The maximum expected torque in the producer well. 25

Figure 5.1 Here entire test bench can be seen with a top view and from the top under an angle. 27

Figure 5.2 The left picture shows the whole bench including the welds. The right picture shows the welds the at the testing section. The belch and the arm setup shown here are not the correct setup. Look at figure 5.6 for an updated version of this setup. 29

Figure 5.3 A picture form the back section taken from the top with its features labeled. 28

Figure 5.4 This shows the testing section with all the parts labelled. 32

Figure 5.5 This show a vertical cross section of the testing section with all the parts labelled. 32

Figure 5.6 This picture shows the belch and pipe system, the pallet weighing scale and the torsion arm. 33

Figure 5.7 This picture shows the hydraulic pump with an insert of the measuring equipment setup. 34

Figure 5.8 The left picture shows the calliper connected to the steel plate. The right figure shows a cross section with the plane at the position of the bearing block. The arm and the displacement whereby the angular displacement φ is calculated are depicted, but are not to scale. 34

Figure 6.1 Stress-strain result of axial tests on date: 12-3-10.. 37

Figure 6.2 Stress-strain result of axial tests on date: 22-3-10 37

Figure 6.3 Stress-strain result of axial tests on date: 21-4-10. Test done with load cell 38

Figure 6.4 Here the hysteresis can be seen in axial direction. 38

Figure 6.5. Stress-strain behaviour of the in the tangential direction of multiple tests. Complete linearity can be observed. 39

Figure 6.6 Two graphs with stress-strain diagrams. From these graphs also the hysteresis behaviour can be seen when the blue and pink lines are compared. The left graph is with 0N axial tension. 41

Figure 6.7 This graph shows the stress-strain behaviour of the shear modulus. Note that after certain stress values all lines show the same tangent 43

Figure 6.8 Shear modulus plotted against the strain under combined testing. Multiple Tests are shown. 44

Figure 6.9 The left graph shows the vibrations of the steel drill string.
The right shows the vibrations of the GRE drill string. Both with a top drive at 40 RPM. 45

Figure 1 Well plan of the producer 54

Table of Tables

Table 6.1 The new dimensions of the casing 40

Table 6.2 The amount of dampening in percentages with the amount of tension applied. 42

Table 6.3 Input data steel and GRE drill string. 44

Table 1 This table gives the build up of the pipe. It shows the type of layer, its weight, volume fraction, its thickness and the direction of the fibres in that layer. 48

Table 2 Here you can find the specification off the materials used in the casing pipe. 48

Table 3 Input data used to calculate the TanD of the producer. 53

Abstract

For the geothermal wells of the Delft Aardwarmte Project it has been chosen to drill with glass-reinforced epoxy (GRE) composite casing in a drilling-with-casing setup. This MSc thesis report describes the results of experimental work to assess the stress-strain behaviour of GRE casing, in particular under axial, torsional and combined axial-torsional loading. These properties have subsequently been used to assess the effects of using GRE casing on standard drilling properties such as the stretch and twist of the drilling tubulars, and the effect on torsional vibrations. The following conclusions can be drawn:

1. For axial loads (in tension) up to 33% of the expected maximum drilling loads:
    a. No evidence was found of non-linear behavior.
    b. The measured elasticity modulus is $1.91*10^{10}$ N/m², which corresponds closely to the manufacturer's data.
    c. The maximum expected elongation of a GRE casing string of 3300 m used for drilling-with-casing is 1.66 m, which is 0.06 m more than that of a steel drill pipe under similar drilling conditions..
2. For torsional loads up to 98 % of the expected maximum drilling loads:
    a. The stress-strain behaviour in the tangential direction remains linear.
    b. The shear modulus measured is deemed incorrect due to the mechanical properties of the test bench. The shear modulus as reported by the manufacturer is $6.78*10^{9}$N/m^2.
    c. The maximum expected twist in a GRE casing string of 3300 m used for drilling-with-casing is 9.25 turns which is 6.3 turns more than that of a steel drill pipe under similar drilling conditions.
    d. The natural frequency in torsional vibration of a GRE casing is much lower than that of a steel casing in a comparable drilling setup due to its much lower torsional stiffness. However the large diameter of casing, as compared to conventional drill pipe, results

in an increase in torsional stiffness. The combined effect is an increased natural frequency of GRE casing compared to steel drill pipe.

e. As a result, the critical rotary speed, i.e the rotary speed below which one can expect the occurrence of stick-slip torsional vibrations, is lower for GRE casing than for steel drilling pipe under similar drilling conditions, i.e. the effect is beneficial.

3. Under increasing axial tension the torsional stress-strain behaviour displays an increasing hysteresis.
    a. The torsional dampening, expressed as energy loss per loading/unloading cycle ranges from xx% to xx%. This is much higher than the typical internal torsional damping in steel drill pipe.
    b. The typical external torsional dampening caused by fluid drag and borehole friction while drilling is in the order of 50%. The effect of internal damping caused by hysteresis during torsional loading of GRE casing is therefore noticeable, and results in a further beneficial decrease in the critical rotary speed for stick-slip torsional vibrations.

1 THESIS OVERVIEW AND OBJECTIVES

The results reported in this thesis were obtained during an assignment to the company Well Engineering Partners (WEP). WEP works in a joint venture named: DIRT (Demonstration INPUT/REGEON technology). DIRT took up the responsibility to develop the composite casing for the Delft Aardwarmte Project (DAP). The goal of this thesis is to investigate the material properties of the composite casing and determine what kind of effect the characteristics have on the drilling process. The properties that were investigated are: the elasticity modulus, shear modulus and the hysteresis. The elasticity modulus will affect the amount of stretch in the drill string. When during drilling it is time to put on a new drill string one has to pull the drill string partly out of the hole to lift the drill bit off bottom. This is especially the case when using a down hole mud motor. If one starts up the motor with the bit being on-bottom the motor can be damaged. To reduce the cost for DAP a single-stand drilling rig (i.e. a rig than can lift the drill pipe out of the hole using only a single piece of pipe a time) had the preference of being used thus limiting the maximum tolerable amount of drill pipe stretch. The amount of stretch in the drill pipe can be calculated with the help of a torque and drag type calculation and requires the drill sting dimension, well plan and of course the elasticity modulus. With the delivery by the pipe supplier, the elasticity modulus and also the shear modulus were reported by the manufacturer, which are $1.54*10^{10}N/m^2$ and $6.78*10^{9}N/m^2$ respectively. The fear for this project was that under increasing loads a different type of stress-strain behaviour could occur that would influence the elasticity modulus, for instance a softening. In this case the drill string stretch might become so large that a two-stand or three-stand drilling rig would have to be used. The first thesis objective was therefore to measure the elasticity modulus (and therefore the axial drill pipe stiffness in tension) and analyse its influence on the expected drill string stretch.

The stress-strain behaviour in the tangential direction (i.e. in torsion) is also measured. Expected is that the resulting shear modulus, and thus the torsional

stiffness, will change when combined with axial tension. The torsional stiffness determines the twist in the drill string, i.e. the number of turns a drill string is torqued up during drilling. A low torsional stiffness, resulting in a large twist, makes it difficult to control the orientation of the down-hole motor and thus complicates the control of the borehole trajectory. Moreover, the shear modulus has an effect on the natural frequency of the drill string for torsional vibrations, The natural frequency of the drill string has an influence on a process that is called stick-slip torsional vibration during drilling, which may slow-down the drilling process and may also damage the drill string connections.. The second thesis objective was therefore to measure the shear modulus (and therefore the torsional drill string stiffness) and analyse its influence on the expected drill string twist and on the natural frequency in torsional vibration.

Finally the hysteresis was tested by dynamically loading the casing in the axial direction, the tangential direction (i.e. in torsion) and then tangentially with increasing axial tension. An increasing hysteresis in torsion results in an increasing amount of dampening of torsional vibrations, and may therefore reduce the chance of getting stick-slip torsional vibrations. The third thesis objective was therefore to measure the hysteresis, especially in torsion, and to estimate the associated amount of damping.

To summarize the objectives:

1. Investigate the stress-strain behaviour under axial loading (tension).
    a. Determine the expected range of axial loading (tension) in drilling operations)
    b. Design a test rig, and supervise construction.
    c. Measure the elasticity modulus.
    d. Asses the influence of the elasticity modulus on the elongation of the drill string.
    e. Set a base case of the axial stress-strain behaviour for combined load testing (paragraph 4.1).

2. Investigate the stress-strain behaviour under torsional loading.
    a. Determine the expected range of axial loading (tension) in drill ing operations)
    b. Design a test rig, and supervise construction.
    c. Measure the shear modulus.
    d. Asses the influence of the shear modulus on the twist of the drill string.
    e. Asses the influence of the shear modulus on the natural frequency of the drill string and the resulting torsional vibrations.
3. Investigate the hysteresis axially and tangentially under increasing axial tension.
    a. Assess the amount of energy lost under hysteresis.
    b. Assess its influence on dampening of the torsional vibrations.

2 General Introduction

2.1 Delft Aardwarmte Project (DAP)

The world is more and more adopting policies to use alternative energies either to be independent from fossil fuels or to be less polluting than fossil fuels. One of these sources is geothermal energy.

DAP is a geothermal project that also aims at innovation. One of these is drilling the geothermal well with a drilling-with-casing technique, using a glass fibre reinforced epoxy (GRE) material. The long term success of this technique is ultimately intimately connected with oil price and environmental issues. If the oil price is going to stabilize at the projected 70 dollars a barrel (date this is written May 2010), the rig rates will again soar because of the fact oil companies will again invest in drilling activities. If this technique succeeds it might be possible to drill geothermal GRE wells with a rotating pile driver, because of the low weight of the composite drill string. This would not only make the drilling much cheaper, but also make the footprint of the needed rig much smaller so that urban drilling would not get so much opposition from surrounding citizens.

The idea is that the well setup would be a doublet (figure 2.1) type with one well acting as the warm water producer and one as the returning cold water injector. The producer well will produce hot water of around 75°C which will be used for city heating of a particular block of houses in Delft and the University itself. Thus the water will directly be pumped through the heating systems of the houses. The returning cooled down water will be injected in the reservoir again. Furthermore, DAP supports the development of geothermal techniques with farmers who produce there products in glass houses.

If this succeeds the next step may be to dissolve CO2 from a conventional power plant in the injecting water and thus increase the green potential of DAP. In figure 1.1 below DAP is schematically shown.

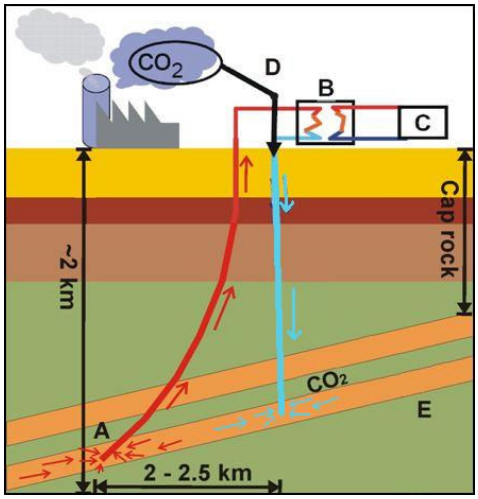


Figure 2.1: Schematically this drawing shows the injector and producer doublet.

2.2 The GRE pipe

2.2.1 Stress-strain behaviour

Previous investigations on the subject of non linear behaviour of laminate structure show that loadings in off axial direction of the fibres show strong non-linear behaviour (Hang, Tsai 1972), (Okihada, Reifsnider 2001) and (Wall et al. 1971). Some studies show non linear stiffening in tension (Gdoutos, Daniel 2008). All previous studies did only testing on structures with fibres in one direction and no structures with multiple directions as in this research. Other research found that a composite cylindrical structure will only show nonlinear behaviour in certain simplified situations (Kocks, Stout 1999) which is not the case here. This thesis will investigate the non-linear stress-strain behaviour of a casing pipe of one manufacturer.

2.2.2 Hysteresis

Hysteresis is defined as the difference in the loading and unloading behaviour. As a consequence a material that displays this hysteretic behaviour experiences a transfer of potential energy (stored in elastic deformation) into heat. Some ways of measuring hysteresis of a certain material is actually by measuring the increase in temperature under cyclical loading and unloading (Hopkins, Williams 1912). Figure 2.2 shows this loading and unloading in a stress-strain graph. This loss of energy can causing damping of vibrations.

Not much research has been done on hysteresis or damping in cylindrical composite structures, and certainly not in composite cylindrical structures with more than two fibre angles or cylindrical structures with different types of fibre layers. Some previous research has been done on finding the correct damping values for the different materials (Bert, 1980), (Gibson 1979). Other research has been done with dampening test using high frequency vibrations from 10Hz up to 60 kHz (Singh, Gutpa 1994). The dynamic testing done in this research will have a frequency around 0.003Hz. This of course is not representative for torsional vibrations down hole, which some research has shown to be around 0.2Hz. The

reason for this is the late realization to try and measure the hysteresis and thus the non preparation in the designing phase of the testing machine. The reason to be insecure about the results gotten here is because of the fact that a composite has different behaviour when loaded with different speeds and especially concerning hysteresis. Although it will give a good indication what the influence of different combined loads will be on the hysteresis.

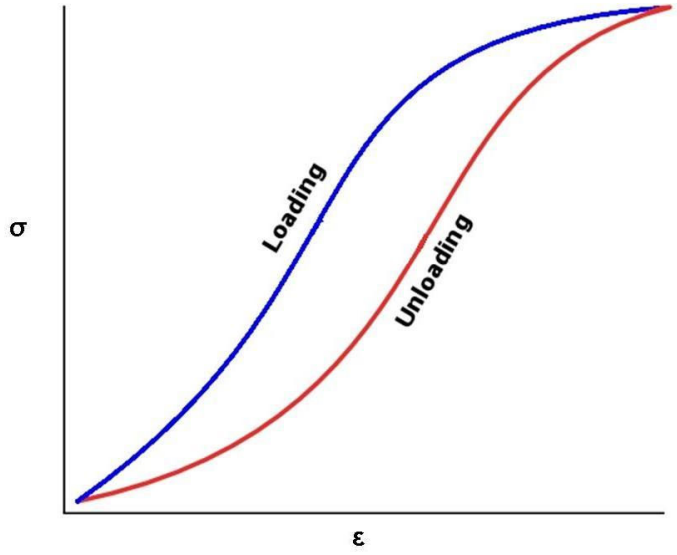


Fig 2.2: Typical stress-strain type graph with a hysteresis profile

2.2.3 The laminate structure

The composite used for this project has especially been designed and produced.. The pipe sections (joints) used to drill to target depth are 9,5m long and have an OD of 188mm and an ID of 160mm. The laminate is built up out of 21 layers of glass fibres. Appendix A has a table were the layers are better defined (table 1). There are three types of layers: random mat, cross layers and unidirectional (UD) tape layer. The random mats are on the outside and on the inside layer. They have short fibres in all directions. They are for protection and do not add much to the behaviour of the pipe. The17° fibres with respect to axial are unidirectional (UD) tape layers are there to cope with the axial tension. These layers are tape that are pre fabricated with fibres in + and - 17° direction. The fibres in this tape are not woven from end to end, but are small fibres all laid in the same direction stitched together with smaller fibres like in figure. The cross layer of 45°, with respect to axial, are rovings of fibres lain from end to end. These layers are there to cope with high torque. The cross layers of 77°, with respect to axial, are there to cope with collapse and burst pressure. The types of fibre and epoxy used can be found in table 2 in appendix A



Fig 2.3: Unidirectional tape on a roll.

3 Torsional vibrations

3.1 Introduction

During drilling the drill string can start showing vibrating behaviour. They can be very damaging to the bottom hole assembly (BHA), drill bit or the well bore. One of the three types of vibrating behaviour that can occur is torsional or rotational vibrations. Torsional vibrations are the oscillations of the drill string around its longitudinal axes. These vibrations start when the rotary table starts rotating. Then the drill string torques up because the static torsional friction at the drill bit and bit face. When enough energy is stored in the string to overcome this static friction the bit it starts rotating. The bit then rotates at speeds higher than the rotating speed of the rotating table. If not stopped, these vibrations will continue during drilling in an oscillating fashion. The characteristics of the vibrations are a function of the geometry, the material, the difference in friction between the static and dynamic friction of the drill bit and bit face and a dampening factor of the drilling fluid (Jansen, van den Steen 1993). No known research has been done on the effect of the dampening properties of the drill string itself. One of the material properties is the shear modulus. For steel, at increasing torque, it will first show a linear relation between shear stress and shear strain (Yoshihara et. al. 1998) before going into its plastic region. As explained in paragraph 1.2.2, for GRE the stress-strain behaviour may also become nonlinear.

3.2 Self-excited vibrations

The vibrations can be represented in a simple model when it is considered that the drill string behaves as torsional pendulum (Jansen 1993), see figure 3.1. Then the drill pipes represent a torsional spring, the drill collars behave as a rigid body hanging from the spring, and the rotary table rotates at constant speed. The corresponding equation of motion is the following:

$$J\frac{\partial^2\varphi_1}{\partial t^2}+c_1\frac{\partial\varphi_1}{\partial t}+k\left(\varphi_1-\varphi_2\right)=T_b,$$

were $J=J_c+\frac{l_{dp}J_{dp}}{3}$ is the equivalent mass moment of the drill collars including the drill string in kgm², $J_c=\rho I_c l_c$ is the mass moment of inertia of the drill collars in kgm² and l_c a unit length of a drill collar in m , $J_{dp}=\rho I_{dp}l_{dp}$ is the mass moment of inertia of the drill pipes per unit length in kgm² and l_{dp} a unit length of a drill pipe in m, were $I_c=\frac{\pi}{32}\left(OD_c^4-ID_c^4\right)$ and $I_{dp}=\frac{\pi}{32}\left(OD_{dp}^4-ID_{dp}^4\right)$ are the polar moments of inertia of the collars and the drill pipes respectively in m⁴, $c_1=\frac{l_{dp}c}{3}$ is the equivalent dampening coefficient in Nms/rad, were *c* is the damping coefficient of the drill fluid per unit length in Ns/rad, $k\frac{GI_{dp}}{l_{dp}}$ is the stiffness of the drill pipes in Nm/rad, with *G* as the shear modulus in N/m², φ_1 is the angular displacement of the drill string in rad, φ_2 is the angular displacement of the rotary table in rad and T_b the torsional friction at the drill bit in Nm.

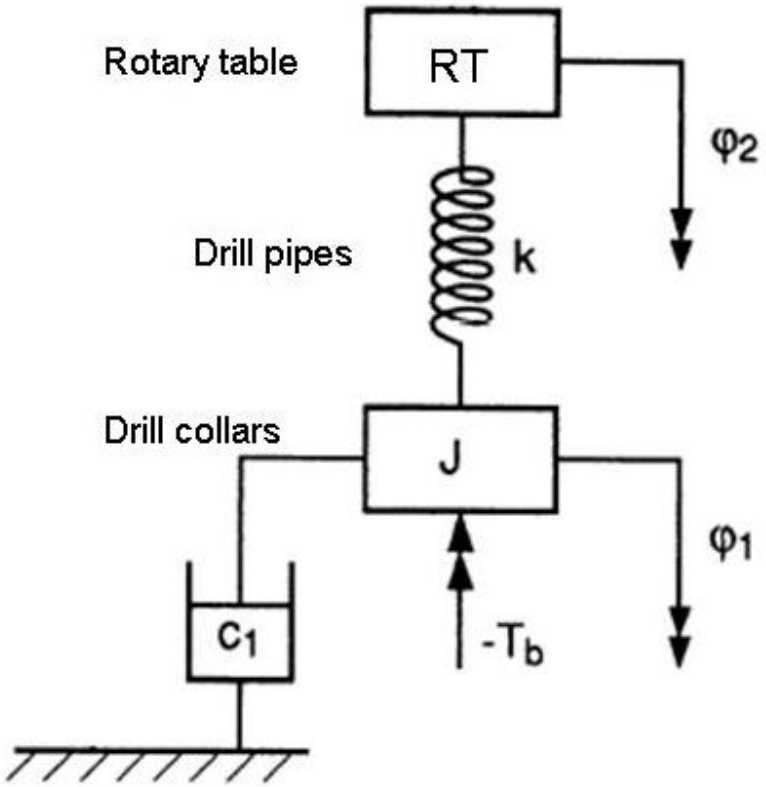


Fig 3.1: Schematic of the drill string as a torsional pendulum. (Jansen 1993).

The above equation of motion is a 2nd order ordinary differential equation which has to be converted to a system of 1st order differential equations in order to model the string behaviour in Matlab. There is a difference in the system whether the sticking-phase is considered i.e. when the drill bit is not moving, or whether the slipping-phase is considered, when the bit is moving. Thus there are two systems of 1st order differential equations. The system of the slip-phase is as follows:

$$\frac{\partial \varphi_2}{\partial t} = \Omega ,$$

$$\frac{\partial \varphi_1}{\partial t} = \vartheta_1 ,$$

$$\frac{\partial \vartheta_1}{\partial t} = -\frac{c}{J}\vartheta_1 - \frac{\kappa}{J}\left(\varphi_1 - \varphi_2\right) + \frac{T_{sl}}{J} ,$$

were Ω is a fixed rotary speed at the top of the drill string in rad/s, ϑ_1 is the drill bit velocity in rad/s and T_{sl} is the generated by the drill bit in the slipping phase in Nm.

The system of the sticking-phase has the following setup:

$$\frac{\partial \varphi_2}{\partial t} = \Omega ,$$

$$\frac{\partial \varphi_1}{\partial t} = 0 ,$$

$$\frac{\partial \vartheta_1}{\partial t} = 0 .$$

The method chosen to solve this equation is with a Matlab ordinary differential equation solver, ODE45. The Matlab code of the whole model can be seen in the appendix B.

4 Torque and drag (TanD)

4.1 Introduction to TanD

To setup a testing regime for the steel/composite glued connections and to have an idea in which range the testing should be performed, the maximum expected axial forces had to be calculated. To calculate these forces in the well a spreadsheet-based torque and drag model was used, based on the torque and drag formulae developed by Johancsik (Johancsik et al. 1984). This model is based on the soft string model. The soft string model is proven to be the most applicable for most well calculations (Mitchel 2009; Samuel 2009). Johancsik divides the drill string in load segments; axial and torsional. Then these segments have to be summed to calculate the total forces. With this method the normal forces need to be calculated per segment first with the help of

$$F_n = [(F_t \Delta\alpha \sin\bar{\theta})^2 + (F_t \Delta\theta + W \sin\bar{\theta})^2]^{\frac{1}{2}},$$

where F_n is the normal force in N, F_t the axial force at the lower end of the segment in N, $\Delta\alpha$ the increase in azimuth angle over the segment length in rad, $\sin\bar{\theta}$ average of inclination over the segment, $\Delta\theta$ increase in inclination angle over the segment in rad and W is the weight of the segment in N. With $\Delta F_t = W\cos\bar{\theta} \pm \mu F_n$ were μ is the friction factor between the pipe and the borehole, we can calculate the axial forces of the chosen segment. When the segments get summed in this fashion $\sum_{i=0}^{N} (\Delta F_t)_i$, this force is the pull up weight of the drill string.

A schematic description of the normal, axial and frictional forces is given in figure 4.1. With $\Delta M_t = \mu F_n r$ the segmental torque can be calculated, with r being the radius of the drill string in m and ΔM_t the increased torque over the segment in Nm. $\sum_{i=0}^{N} \Delta M_i$ gives the maximum torque generated by the drill string.

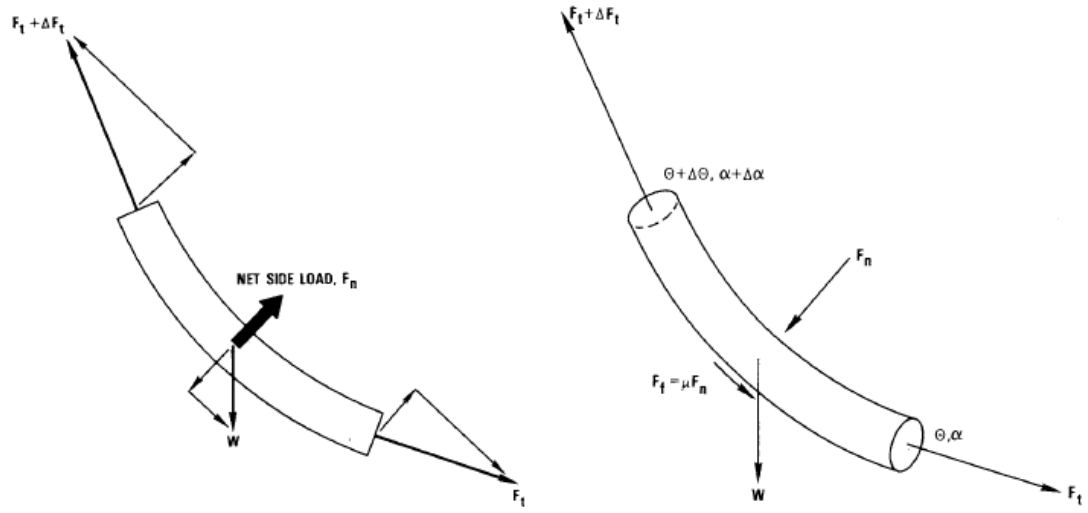


Fig 4.1: The left figure shows a schematic of the forces in on the hole giving an overall net side load of F_n. The right side shows the force distribution when pulling out of the hole (Johancsik et al. 1984)

A detailed description of these equations can be found in the appendix C. The next section will give the results of the TanD calculations.

4.2 TanD Results

4.2.1 Results of the TanD analysis

These analysis were done very early in the DAP project to setup load cases for a testing regime for the connection and for the behaviour of the GRE. During this project already changes have been made to the well design. The results are shown only for the second $7^{5}/_{8}$" section to target depth (TD). The load cases for this section have been used because this section has the highest loads which were used for the development of the connection. On top of that, this section is also the only section that will be tested for its behaviour as the development process didn't allow for more time to test on the bigger top section pipes.

4.2.2 The $7^{5}/_{8}$" section to TD

The density of the GRE in this modelled case is 2600kg/m³, which is way too much. In reality the GRE drill string including the steel connections is 1339km/m³. When this project was started on this project not much was known about GRE so the density of glass (2600kg/m³) was chosen to be sure not to underestimate the maximum loads. Further parameters are in appendix for review. It can be seen in figure 4.2 that the drill string in the producer well may experience forces up to but not exactly 450000N pull up weight. The value of 450000N has been chosen as maximum axial load just to be sure. The graph in figure 4.2 shows the maximum torque built up in the drill string, which is 15000Nm. This is the maximum expected torsional load. You can see that the torque starts at 5000Nm at TD, This is because this is the torque needed by the mud motor which will be used is around 5000Nm. Note the change in tangent at 1000m depth were the kick off point is. So now the two values are know by which the whole testing sequence can be setup for first the testing of the connection and second the stress-strain testing.

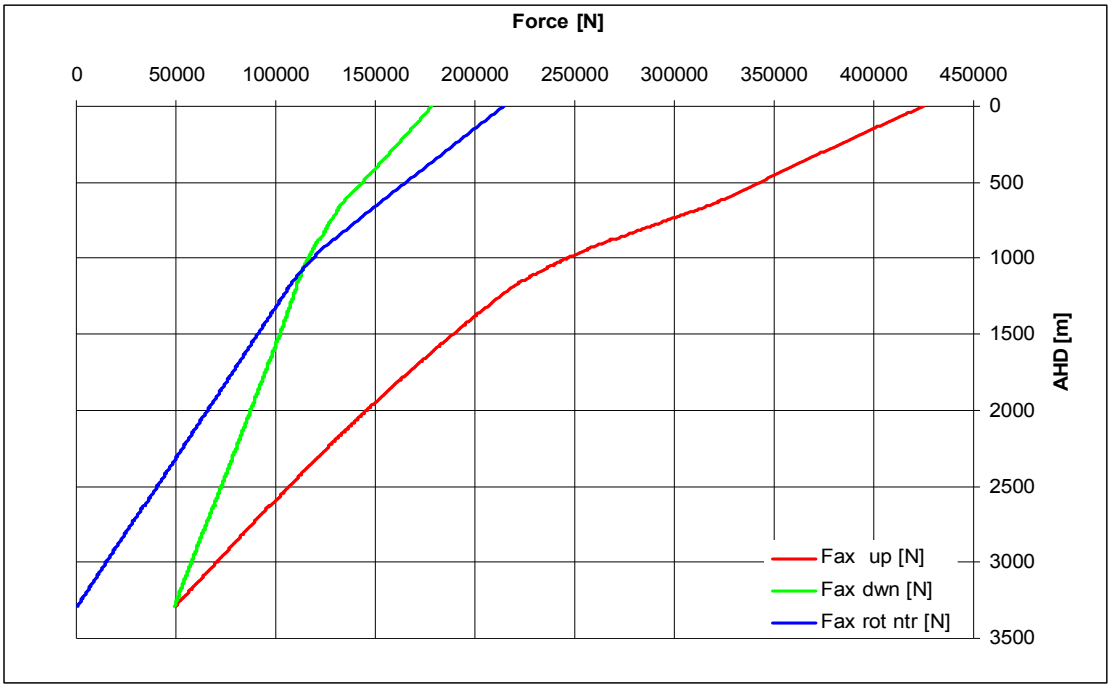


Fig 4.2: This graph shows the maximum expected forces in the producer well.

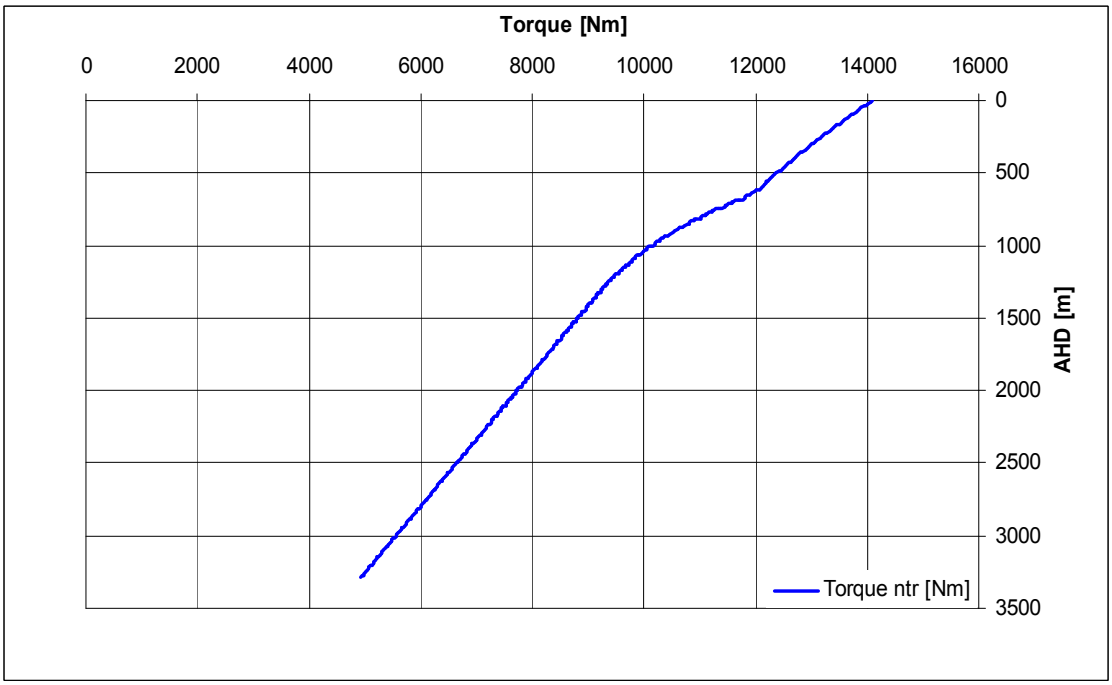


Fig 4.3: The maximum expected torque in the producer well.

5 Stress-strain testing methods

5.1 Testing stress-strain behaviour

The stress-strain behaviour was tested in two directions; axial and tangential. Also the stress-strain behaviour of the two directions combined. First the stress-strain behaviour was tested in the axial direction. Then in the tangential direction by putting torsion on the pipe. The combined loading will be done to see how the behaviour of both directions will translate in the behaviour of the two loads combined.

For sake of later calculation in drilling software and for simplified communication the stress-strain behaviour in the axial direction will be called the elasticity modulus. Technically this is not entirely correct, because the fibres in the pipe are not all in axial direction.

5.2 Testing hysteresis

The hysteresis was tested by loading and unloading the pipe in axial direction and by loading and unloading the pipe with torque. Then the hysteresis was tested in the tangential direction combined with axial tension, whereby the axial tension was stepwise increased. The data was then put into a stress-strain diagram.

The testing was done on the whole system. i.e. the elasticity modulus and shear modulus and these characteristics combined are computed from measurements taken over the whole system: steel box and pin, the GRE pipe and the adhesive between the pipe and the box and pin. Here the assumption is made that the adhesive and steel box and pin have infinite stiffness.

5.3 The test bench

The basic structure of the bench is built up out of four u-shaped UNP 400 S235 JRG2 steel beams to make the basic rectangular structure seen in figure 5.1. This is the “chassis” to which the rest of the parts are mounted. The maximum force that would be delivered was 60 tons. The corresponding axial stress, for a surface area of 9150mm² per beam, was therefore 32 N/mm². The yield strength of the UNP beams is 235 N/mm². The chassis was placed on small steel plates (fig 4.1 & 4.2) that were welded to the floor. Also the cross beam were welded inside the chassis to prevent the whole chassis from bending. The location of the welds can be seen in figure 5.2. The plates provide stability, level out the chassis and it prevent the chassis from bending when torsion is put on the pipe.

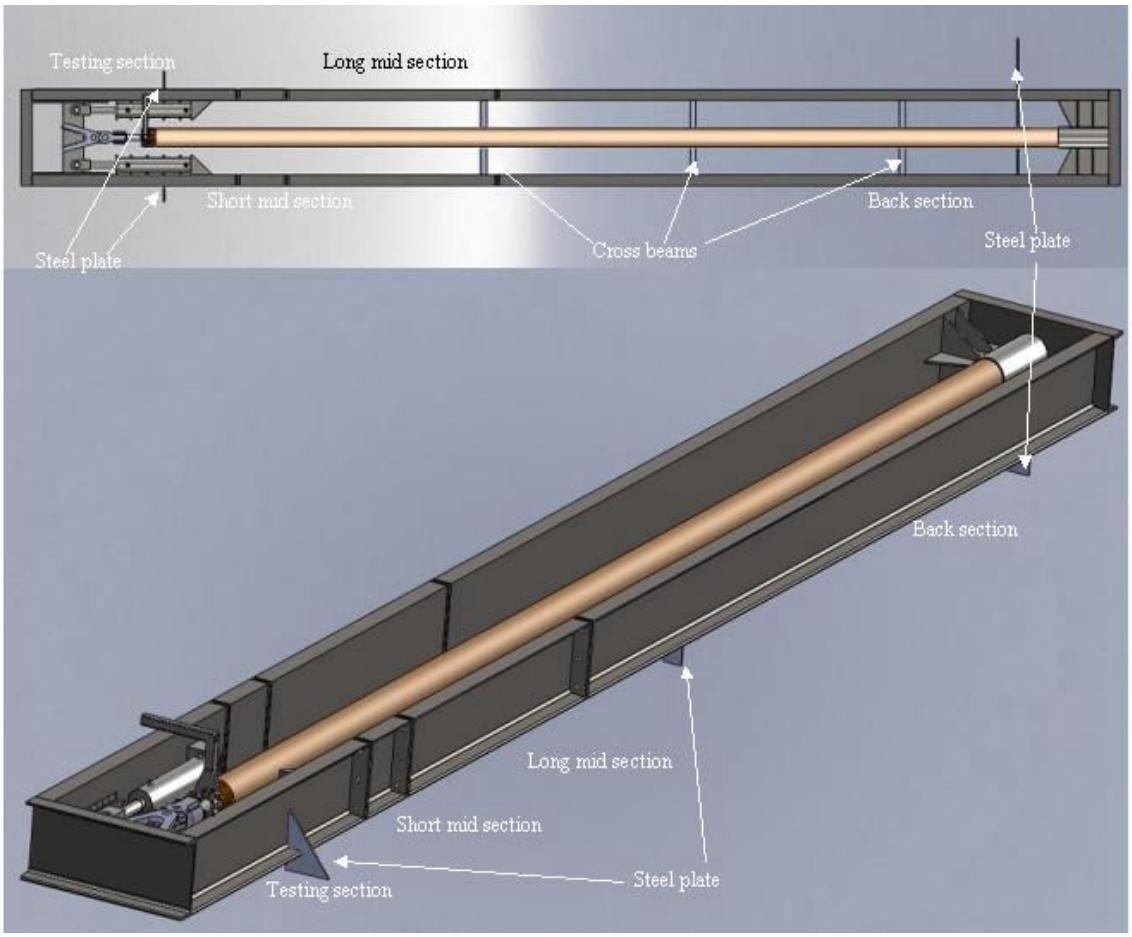


Fig 5.1: Here entire test bench can be seen with a top view and from the top under an angle.

The bench is divided in four main sections displayed in figure 5.1: the back section, the long mid section, the short mid section and the testing section. The back section is were the pipe is screwed into a box which is welded to the back of the section and is supported with steel plates to make sure the box does not twist under torsion. The mid section consists of two steel beams to increase the length of the bench to accommodate the length of the pipe. The reason to use different sections is because the bench has a secondary testing function The secondary testing function which uses only the back end and the testing section is for another project within DAP and is not described here. The short mid section had to be put in because an employee miscalculated the length of the total mid section. The testing section is the section were the torsion and the tension is put on the pipe. It also houses the measuring equipment. The testing section is described in more detail in the next chapter.

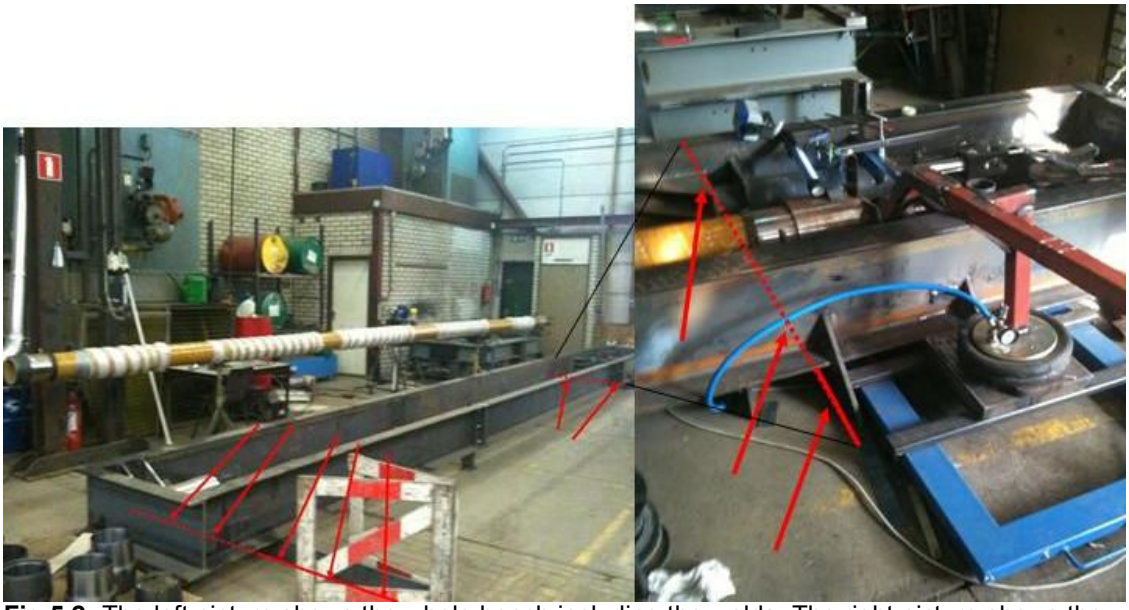


Fig 5.2: The left picture shows the whole bench including the welds. The right picture shows the welds at the testing section. The belch and the arm setup shown here are not the correct setup. See figure 5.6 for an updated version of this setup.

5.3.1 The testing section

The placement of two cylinders can be seen in figures 5.1 & 5.3. These cylinders have a plunger diameter of 130 mm and can handle a maximum pressure of 300 bar. The pressure is delivered with a Hobo hydraulic pump (figure 5.7) with a pump that turns at 1000 RPM and a pump rate of 0.41 cm³/min. The pressure in the cylinders is measured via an Intab pressure sensor at the exit of the hydraulic pump. This pressure sensor is hooked up to a data-logging device that converts the analogue signal to a digital signal. This digital signal can then be viewed real time and is converted to pressure on a laptop with Easyview software. The cylinders push the rectangular plate which then delivers the axial tension through hook and link to fork end to a steel axle. The steel axle is screwed into to a block which in turn is screwed into the box on the pipe. Figures 5.3, 5.4 & 5.5 show these parts in a picture and in two Solid Works figures. So when the cylinders push the rectangular block stress is put onto the pipe axially. The caliper in figure 5.3 measures the elongation.



Fig 5.3: A picture form the back section taken from the top with its features labeled.

The steel axle is hold in place by a bearing block, so when torsion is put onto the pipe it will stay centered. The bearing inside the bearing block can take a maximum dynamic load of 156 kN radially. If the pipe has unlimited stiffness, the delivered torque would be delivered directly to the bearing radially. The maximum applied load here was 15000 Nm,so the bearing was more than able to take 15 kN. A safety factor of 1.5 on top of the 15 kN could not be applied because this was mechanically not possible because of the then very long stroke that would occur. It would have been be a to costly operation to make this possible. The way the force is delivered for the torque is by two belches stacked on top of each other. A data sheet of the type of belch is put into the appendix D. The reason for two belches and not one is the fact that one belch could not deliver the stroke needed to rotate the pipe to the extent in this experiment. To keep the belches together they were fitted inside a 300mm (inner diameter) PPE pipe coated with a lube so the belches would slide along the inner wall of the PPE pipe when expanding upwards. The belch and pipe unit is kept in place by steel girdles which are welded to a rack seen in figure 5.6. This rack had the possibility to be angled with a thread and nut so that the top belch had the optimum position to the foot of the arm. This foot is inside the pipe and cannot be seen in figure 5.6. The angle was needed because the top belch had the tendency to bend around the foot of the torsion arm and so wanted to pop out of the pipe. The rack was kept in place by two gluing clamps onto the pallet weighing scale. This weighing scale is connected to a readout unit that can be seen in the insert in figure 5.7. The read out was placed near the calliper so that a camera could shoot the weighing scale readout and the calliper (figure 5.7) in one shot.

The mechanism by which the torque is delivered onto the pipe can be seen in figures 5.4 & 5.5. The arm is welded onto a plate with 7 holes. The axle centres the plate and the nut fixates the plate into the block. The block has 6 holes. The combination of 6 and 7 holes makes for almost unlimited combinations for the plate and the block to have at least one hole line up so the nut can go through and subsequently the arm would be in the lowest position so the maximum stroke

could be reached. The reason for this technique was the fact that the block had to be screwed into the box of the pipe, after which the holes can be at any place. The actual testing of the stress-strain behaviour in the axial direction was done by gradually increasing the pressure in the cylinders. The pressure could be read in the Easyview software after the pressure was stabilized. At the same time elongation was noted from the calliper. Both values were then put into an Excel file for later analysis. During the design phase of the GRE pipe including the glued connection a safety factor of 1.5 was chosen on top of the 45tons that were calculated in paragraph. 3.2.2. The whole GRE project has from then on been engineered from the 67.5tons. The maximum axial tension chosen for this experiment had to be 60ton. The reason not to go above 60ton is because or the fact that the box and pin that were glued to the pipe hadn't been glued under optimum temperature conditions. Furthermore the glued connection was far from perfected. The stress-strain behaviour axially was tested by first increasing the pressure, whilst reading out the pressure and elongation and then gradually decreasing the pressure and then reading of the elongation.

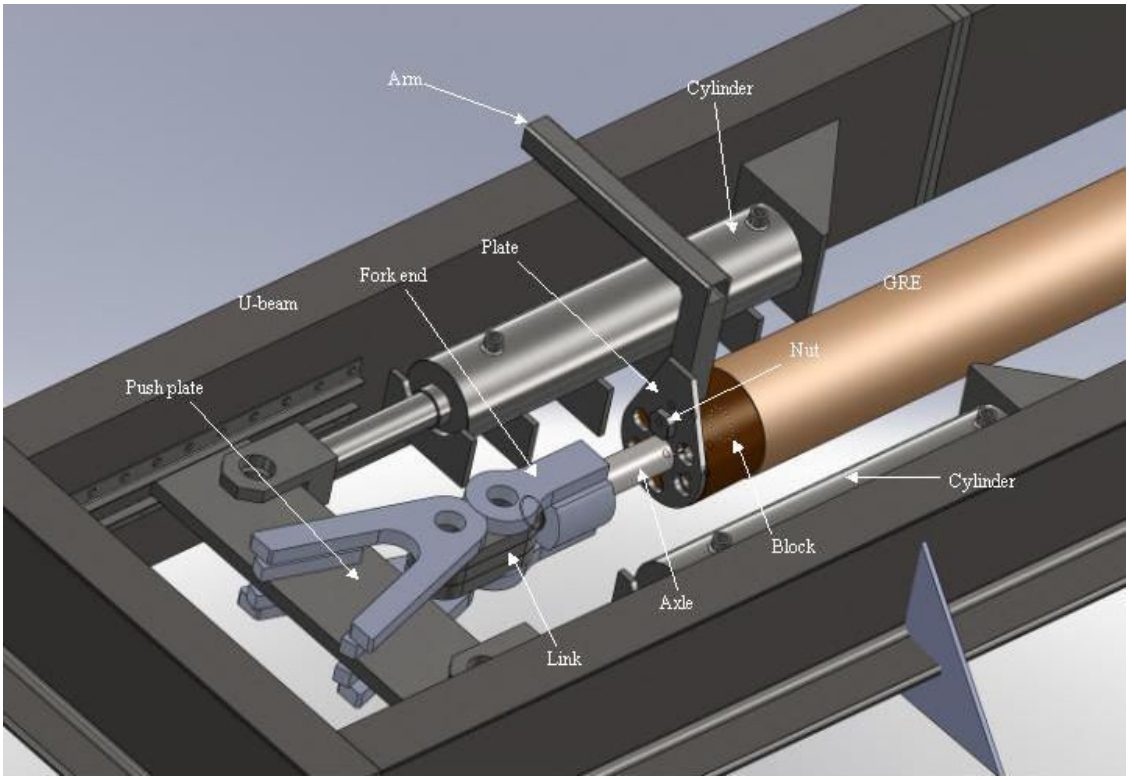


Fig 5.4: This shows the testing section with al the parts labelled.

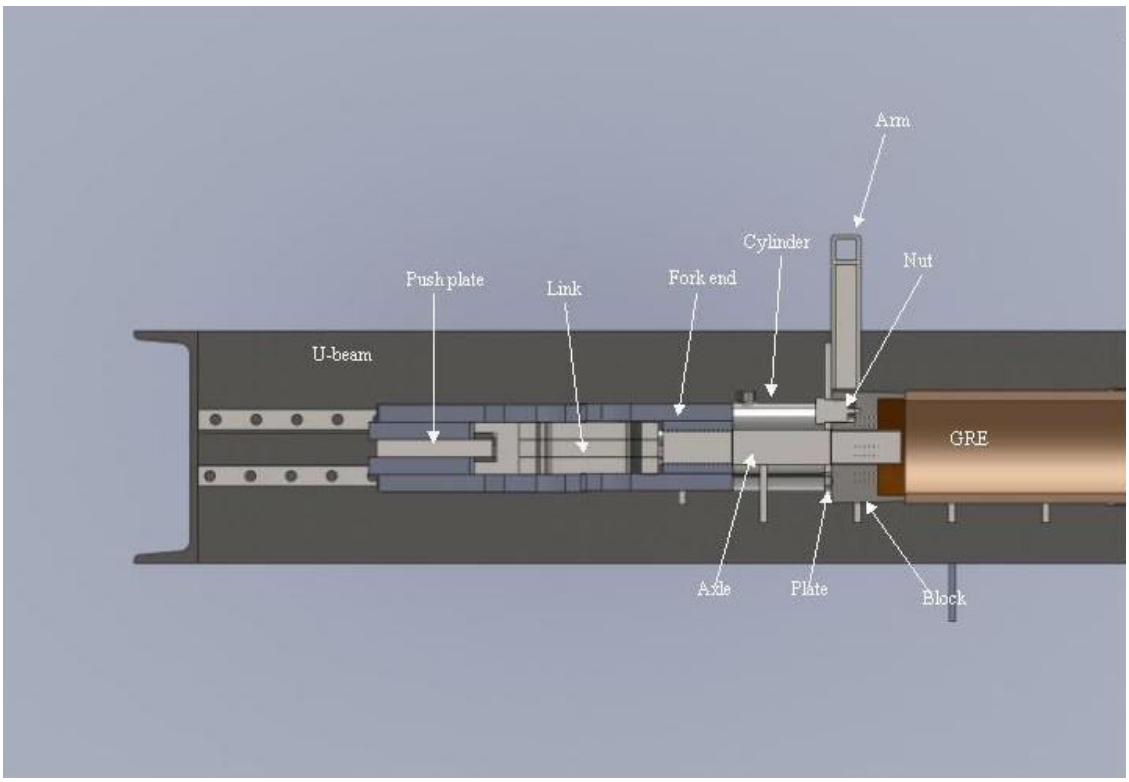


Fig 5.5: This show a vertical cross section of the testing section with all the parts labelled.

Because of the fact that the decreasing of the pressure couldn't be measured correctly by the pressure sensor a load cell was used. Due to structural limitations only a 25ton load cell could be rented. Now the axial force was read of from the load cell. The load cell replaced the link.

The stress strain behaviour in the tangential direction was measured by increasing pressure inside the belches. The belches were linked to each other by tubing so that they would automatically even the pressure. This increase in pressure made the arm go up which in turn put torque on the pipe. The amount of force delivered to the arm (fig 4.7) was measured by the weighing scale in kilograms. This amount could be read a remote read out. The angular displacement was measured by measuring the displacement of the small steel plate (fig 4.8) to which the end of the calliper is connected with a magnet. The magnet holds the metal of the calliper in place so when a dynamic test is done it pulls the calliper back as well. With a known height of the small steel plate and the displacement the angular displacement can be calculated (fig 4.8).



Fig 5.6: This picture shows the belch and pipe system, the pallet weighing scale and the torsion arm.

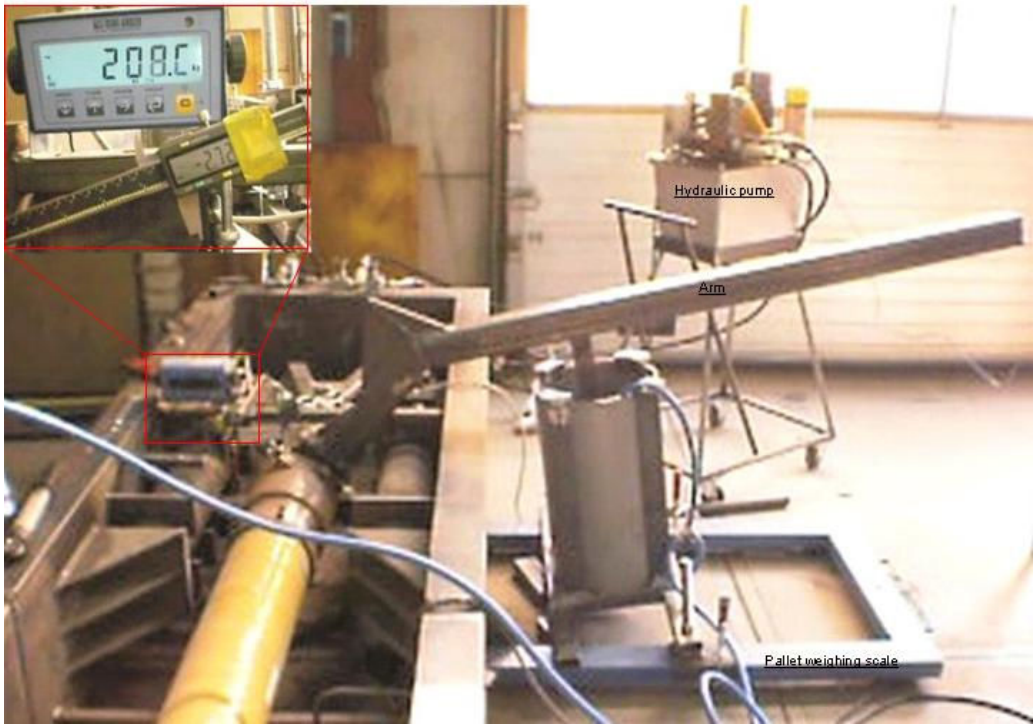


Fig 5.7: This picture shows the hydraulic pump with an insert of the measuring equipment setup.

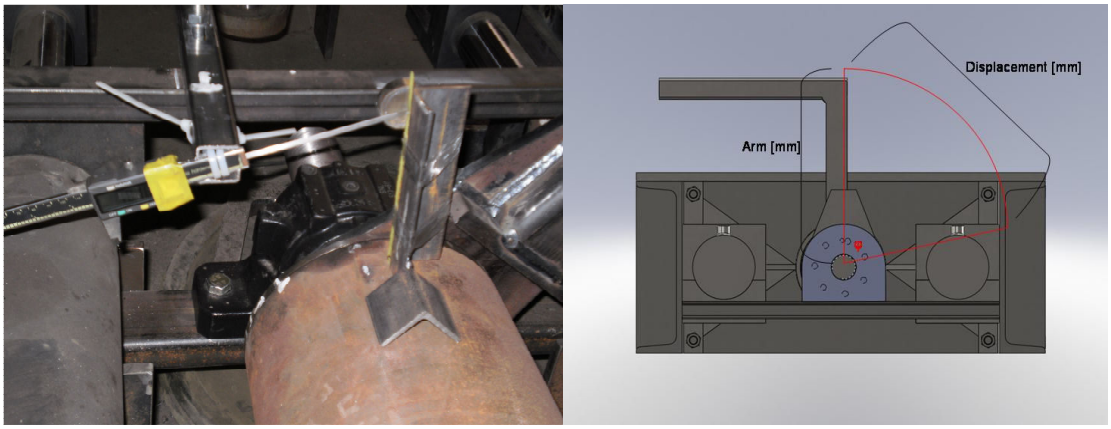


Fig 5.8: The left picture shows the calliper connected to the steel plate. The right figure shows a cross section with the plane at the position of the bearing block. The arm and the displacement whereby the angular displacement φ is calculated are depicted, but are not to scale.

5.4 Calculating the elasticity and the shear modulus

The elasticity modulus from these results was calculated with equation

$E = \frac{d\sigma}{d\varepsilon}$, with $\sigma = \frac{F}{A}$ and $\varepsilon = \frac{\Delta L}{L}$, were E is the elasticity modulus in N/m², *F* is the applied force in the direction of the elongation in N, *L* is the original length of the object in m, *A* is the original surface area of the object perpendicular to the elongation and ΔL is the elongation in m. In this case of testing the input parameters for the above equations are the force which is controllably put in and the elongation which is a result of this force. The elasticity modulus is calculated by approximating $E = \frac{d\sigma}{d\varepsilon}$ with $E = \frac{\Delta\sigma}{\Delta\varepsilon}$.

The shear modulus from these results is calculated through equation

$G = \frac{d\tau}{d\gamma}$, with $\tau = \frac{rM}{I_p}$ en $\gamma = \frac{r\Delta\varphi}{L}$ where *r* is the distance from the centre of the pipe, φ is the angular displacement in radians, *M* is the torque in Nm, *L* the length of the cylinder in m, *G* is the shear modulus in N/m² and Ip the polar moment of inertia in m⁴. In the case of the shear modulus the input parameters are the torque and its dependent variable the angular displacement. The shear modulus is calculated by approximating $G = \frac{d\tau}{d\gamma}$ with $G = \frac{\Delta\sigma}{\Delta\varepsilon}$.

6 Results

6.1 Results of stress-strain behaviour of the axial direction

As the stress-strain behaviour axially shows strange results it will be presented as follows; the testing was done on three days therefore three graphs have been produced with the day's measurements. Figure 6.1 shows tests done on the date 12-3-10 with four test, t6, t7, t8 and t9. Earlier tests results and t17 were deemed unfit due to clear technical problems. Tests t6, t7 and t8 show a clear linear trend. However t9 shows a steeper trend and an additional stiffening at a stress of $6.5*10^7 N/m^2$. This implies that the pipe is stiffening. If this was indeed the case, this effect should have been seen in every subsequent test, because of the fact that when a GRE material changes its properties due to for instance relaxation, it is definite. This relaxation would have been accompanied by acoustic emissions (hard snapping sound) from inside of the material according to the manufacturer. Which was not the case. So looking at the test results of the dates 22-3-10 (fig 6.2) and 24-4-10 (fig 6.3), this behaviour indeed is not subsequent. For instance in the case of t10, t11 and t12 it can be seen that the stiffening with t11 does not occur again with t12. On top of that t11 shows a much stiffer behaviour than t13 till t16. These differences do not give enough confidence that the test material is indeed stiffening. The most obvious reason for this stiffening trend is the fact that the push beam dug itself into the U-beams. Later inspection confirmed damaged U-beams. Figure 6.3 shows two axial tests done with a load cell. For further calculations these measurements are the most precise and deemed correct because the push beam, although sometimes digging into the U-beams, were supported by only the fork ends. This means that the push beam experienced no friction when freely moving forward.

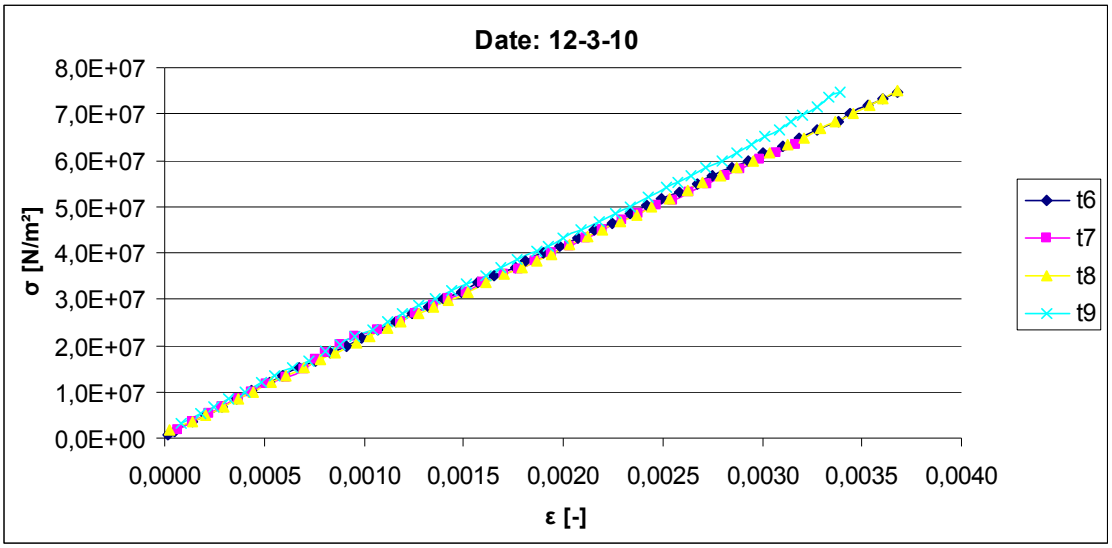


Fig 6.1: Stress-strain result of axial tests on date: 12-3-10.

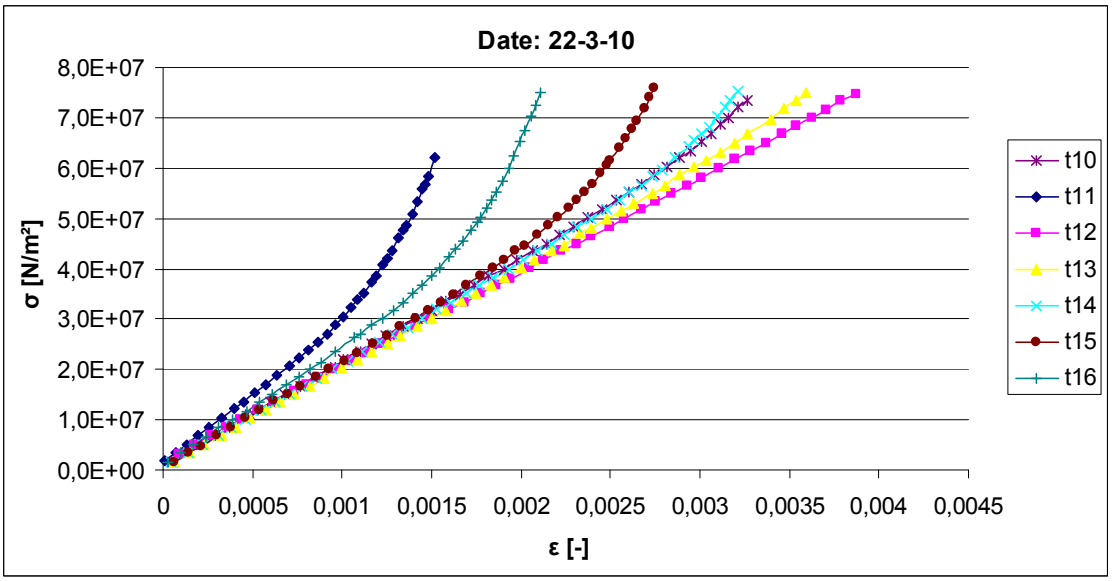


Fig 6.2: Stress-strain result of axial tests on date: 22-3-10.

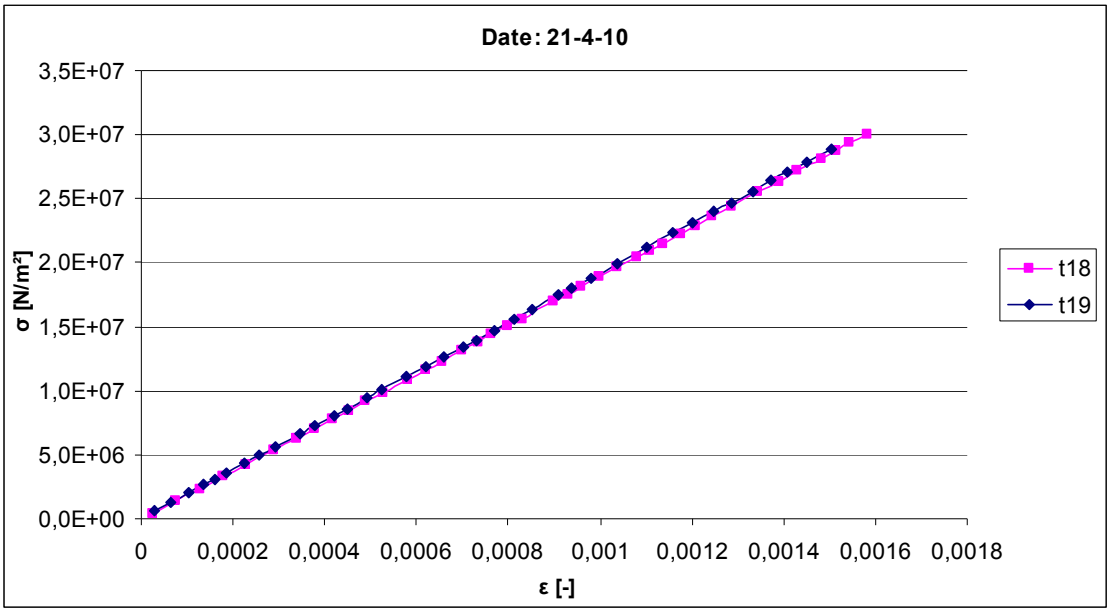


Fig 6.3: Stress-strain result of axial tests on date: 21-4-10. Test done with load cell.

In figure 6.4 the hysteresis can be seen in the axial direction of the pipe. It shows that there is hysteresis and thus an amount of dampening. It has to be noted here that this test has only been done up to a force of 250kN. The reason for this is the fact the load cell could not take higher loads.

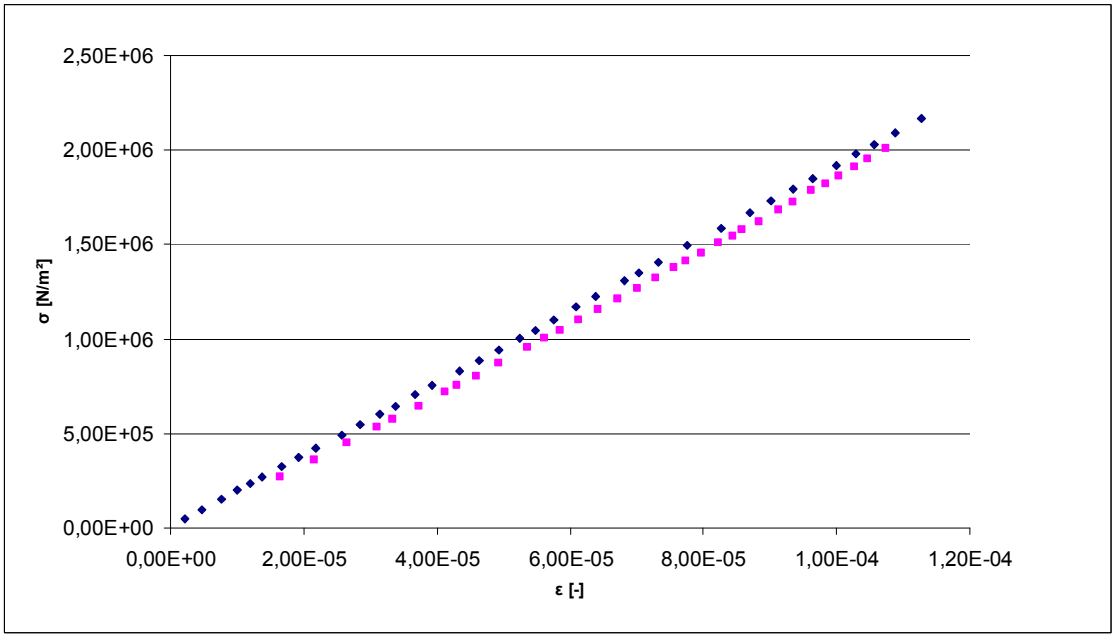


Fig 6.4: Here the hysteresis can be seen in axial direction

6.2 Results of the tangential stress-strain behaviour.

Figure 6.5 illustrates that there is no non linear behaviour to be seen when testing the shear modulus. The calculated shear modulus from this graph is $7.3*10^9 N/m^2$. Due to the fact the arm shown in figure 5.7 has mass, it influences the measuring of the force, thus overestimating the shear modulus by 8%.

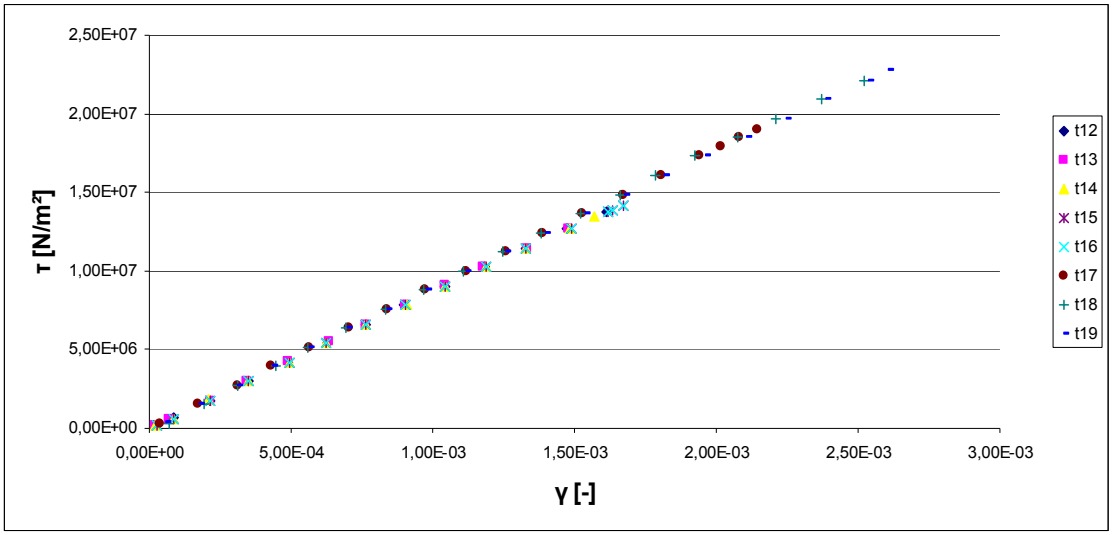


Fig 6.5: Stress-strain behaviour of the in the tangential direction of multiple tests. Complete linearity can be observed.

6.3 The elongation and twist of the drill string

To calculate the elongation when pulling out the drill string the same torque and drag spreadsheet has been used as in chapter 4. At the moment of writing this the dimensions of the pipe and connection have been changed. These new dimensions are shown in table 6.1. The chosen elasticity modulus has been calculated from t19 as this was measured with the load cell and is deemed more precise than the given value of the manufacturer. From the stress-strain graph of t19 an elasticity modulus of $1.91*10^{10}N/m^2$ has been calculated by taking an average from all elasticity moduli calculated as mentioned in paragraph 5.4 over all data points. This value is 24% higher than the value given by Fiberdur. Experts say that the theoretical calculated strengths are sometimes not exactly reached in the manufacturing process.

New input data	Value	Units
Density per section inluding steel box and pin	1339	**kg/m³**
Pipe ID	6,3	**inch**
Pipe OD	7,45	**inch**
Pipe OD coupling	8,63	**inch**
Elasticity modulus	1,91E+10	**N/m²**
Shear modulus	6,78E+09	**N/m²**
Fax up elongation	1,66	**m**
Fax down elongation	0,76	**m**
Fax rotating elongation	1,09	**m**
Twist	9,25	**turns**

Table 6.1: The new dimensions of the casing

The data here is calculated for the Fax up, Fax dwn and Fax rotating, were the elongations are 1.66m, 0.76m and 1.09m respectively. These are values that don't give any concerns off getting into trouble with the drilling operations. The shear modulus chosen here is the shear modulus the manufacturer gave. The reason for this is stated in paragraph 6.2. The shear modulus affects the twist in the drill string measured noticed in twist at the top. This case has been modelled with a mud motor. A mud motor is a device that sits at the end of the drill string with a drill bit attached. The mud that is pumped down the drill string drives the motor. This motor delivers a torque of 5000Nm at the drill bit. The maximum torque at the rotary table is this torque combined with the friction generated by

the drill string and the bore hole. When accurate steering of the mud motor is required it is preferred to have not to rotate the mud motor. This also means the drill string is not rotating. So what has to be done keep the motor from turning is to turn the drill string a certain amount of times so that the torque delivered with the motor is being countered by turning the drill string. In this case 9.25 turns. This won't be a problem as it is normal procedure to account for the torque of the mud motor with this amount of twist in the drill string.

6.4 Tangential stress-strain behaviour combined with axial tension

The characteristics looked for here are nonlinearity in the shear modulus and hysteresis under increasing axial tension. Let us first look at the results first before commenting on these unexpected results. Below in figure 6.6 two graphs are placed one were the shear modulus is measured at 0 N axial tension and one at the maximum axial tension of 459254 N. Appendix D shows all results of the hysteresis test.

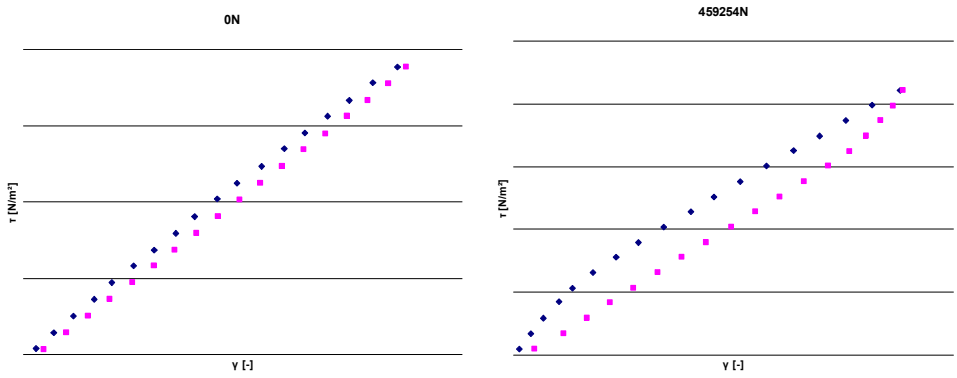


Fig 6.6: Two graphs with stress-strain diagrams. From these graphs also the hysteresis behaviour can be seen when the blue and pink lines are compared. The left graph is with 0N axial tension on the pipe and the right is with 459254N axial tension on the pipe.

Tension [N]	Dampening %
0	
53093	
106186	
159279	
212372	
265465	
325194	
376960	
431380	
459254	

Table 6.2: The amount of dampening in percentages with the amount of tension applied.

What is very much unexpected from these results is the fact the hysteresis increases at the same time the axial forces on the pipe increase. Table 6.2 shows the amount off energy loss/dampening that occurs under a specific load. These have been calculated by calculating the surface area between the loading and the unloading with the trapezoidal rule.

What also can be seen in the stress-strain is small non linearity, but this time only under axial tension seen in figure 6.7. In figure 6.8 the shear moduli of 10 tests are plotted with t1 under 0N axial tension and t10 under 459254N axial, were this small non linear behaviour can also be seen. After this small non linearity all tests reach the same value of shear modulus. This is better illustrated in figure 6.8,

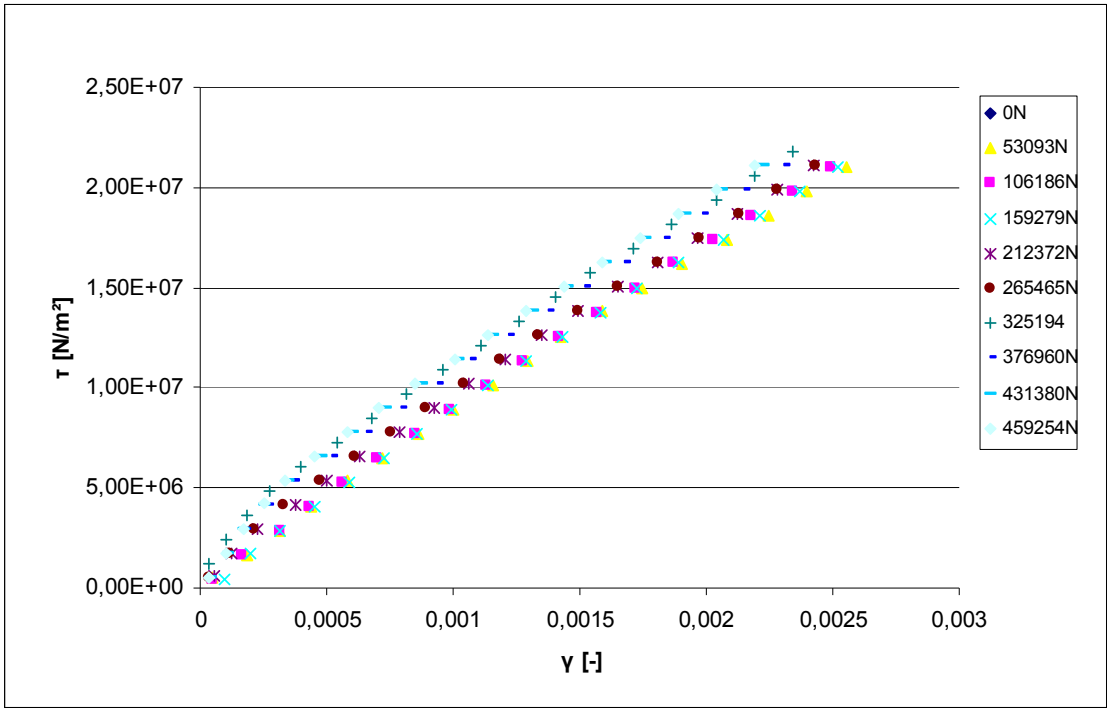


Fig 6.7: This graph shows the stress-strain behaviour of the shear modulus. Note that after certain stress values all lines show the same tangent and thus the same shear modulus.

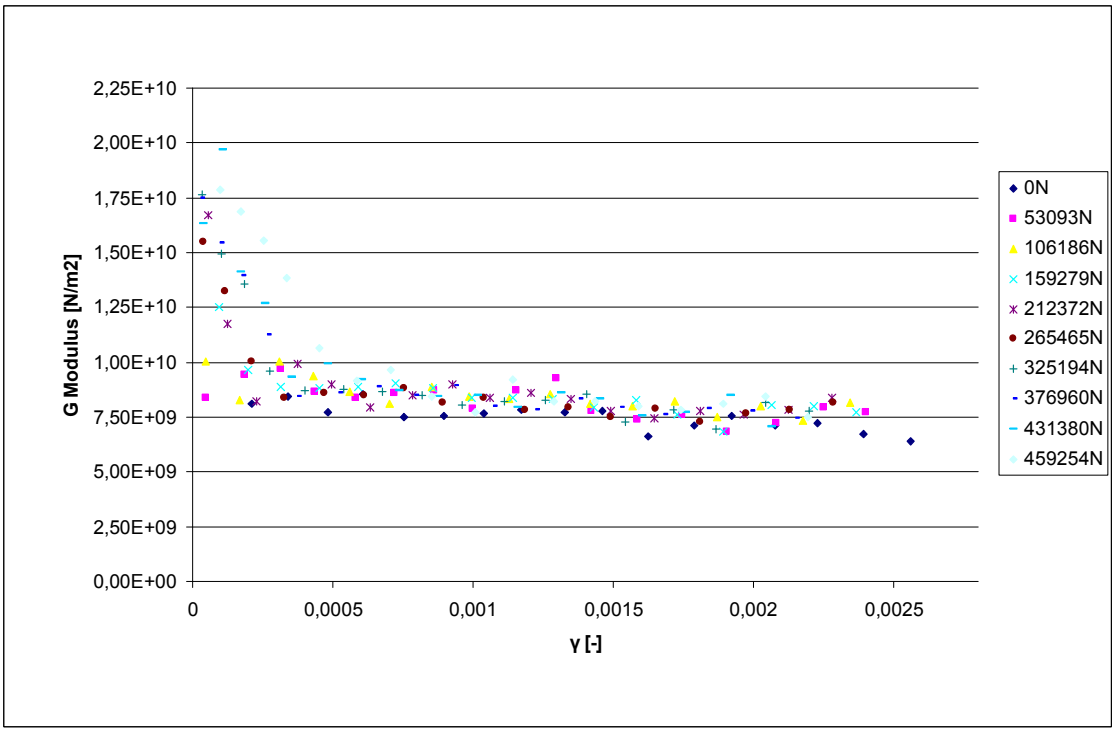


Fig 6.8: Shear modulus plotted against the strain under combined testing. Multiple tests are shown.

6.5 A comparison between GRE and steel concerning torsional vibrations

To illustrate what effect the properties of the GRE have on torsional vibrations a comparison between a steel and GRE drill string has been made. Table 6.3 shows the drill string data.

		Steel	GRE	GRE Casing	
Drill pipe	**OD**	5	5	7,45	**inch**
	ID	4,3	4,3	6,30	**inch**
	Length	2000	2000	2000	**m**
	G	7,93E+11	6,78E+09	6,78E+09	**N/m²**
	rho	7850	1339	1339	**kg/m³**
Drill collar	**OD**	9	9	7,45	**inch**
	ID	3	3	6,30	**inch**
	Length	150	150	100	**m**
	rho	7850	7850	7850	**kg/m³**
	G	7,93E+11	7,93E+11	7,93E+11	**N/m²**
	Tsl	2000	2000	2000	**Nm**
	Tst	4000	4000	4000	**Nm**
Output	**J_dp**	0,09	0,025	0,082	**kgm**
	J_c	2,1	2,1	0,48	**kgm²**
	J	372	322	127	**Nms²/rad**
	k	458	48	208	**Nm/rad**
	w	1,11	0,39	1,43	**rad/s**
	Ωcrit	48	66	13	**RPM**

Table 6.3: Input data steel and GRE drill string.

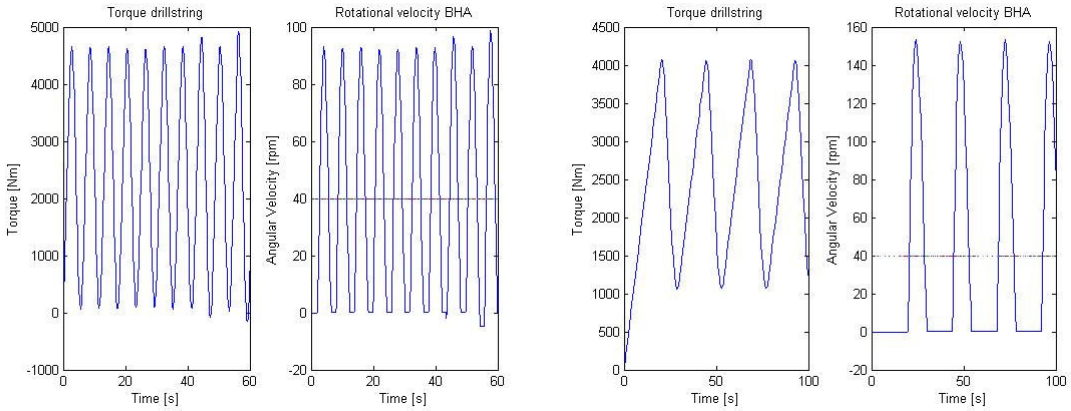


Fig 6.9: The left graph illustrates the vibrations of the steel drill string. The right graph shows the vibrations of the GRE drill string. Both with a top drive at 40 RPM.

What can be observed from the table is that the lower shear modulus has the greatest effect on the output data. The output data that is the most affected by the different properties of the GRE is the stiffness *k.* This is due to the lower

shear modulus of the GRE. Compared to the shear modulus the lower weight has little effect due to the massive weight of the collars. The stiffness thus also has a bigger effect on the natural frequency of the drill string. Because of this lower stiffness it can take a greater angular displacement before it torques up enough to reach the sticking torque point. This can be seen clearly in figure 6.10 were lower frequency vibrations can be observed. Another observation is that the GRE has a higher critical rotary speed whereby the drill string dampens out. Looking at a casing drilling setup, whereby the drill pipe have the same dimensions as the drill collars, it can be seen that the increased OD of the drill pipe increases the stiffness of the drill sting and subsequently increases the natural frequency of the pipe and thus the critical rotary speed whereby the drill string dampens out.

6.6 Damping due to hysteresis.

Here a small case is made on how much the hysteresis influences the damping on the torsional vibrations. As the hysteresis increases more or less linearly with an increasing axial tension the amount of hysteresis can be averaged over the drill string. This amounts to $average_damping = (Min_h + Max_h)/2$ were Min_h is the minimum hysteresis and Max_h is the maximum hysteresis. The calculated damping from the measured hysteresis is 13.8%. The typical external torsional dampening caused by fluid drag and borehole friction while drilling is in the order of 50%. The effect of internal damping caused by hysteresis during torsional loading of GRE casing is therefore noticeable, and results in a beneficial decrease in the critical rotary speed for stick-slip torsional vibrations.

7 Conclusions and recommendations

7.1 Conclusions

Referring back to the objectives the following conclusions can be made.

1. For axial loads (in tension) up to 33% of the expected maximum drilling loads:
    a. No evidence was found of non-linear behavior.
    b. The measured elasticity modulus is $1.91*10^{10}$ N/m², which corresponds closely to the manufacturer's data.
    c. The maximum expected elongation of a GRE casing string of 3300 m used for drilling-with-casing is 1.66 m, which is 0.06 m more than that of a steel drill pipe under similar drilling conditions..
2. For torsional loads up to 98 % of the expected maximum drilling loads:
    a. The stress/strain behaviour in the tangential direction remains linear.
    b. The shear modulus measured is deemed incorrect due to the mechanical properties of the test bench. The shear modulus as reported by the manufacturer is $6.78*10^{9}$N/m^2.
    c. The maximum expected twist in a GRE casing string of 3300 m used for drilling-with-casing is 9.25 turns. which is 6.3 turns higher than that of a steel drill pipe under similar drilling conditions.
    d. The natural frequency in torsional vibration of a GRE casing is much lower than that of a steel casing in a comparable drilling setup due to its much lower torsional stiffness. However the large diameter of casing, as compared to conventional drill pipe, results in an increase in torsional stiffness. The combined effect is an increased natural frequency of GRE casing compared to steel drill pipe.
    e. As a result, the critical rotary speed, i.e the rotary speed below which one can expect the occurrence of stick-slip torsional vibrations, is lower for GRE casing than for steel drilling pipe under similar drilling conditions, i.e. the effect is beneficial.

3. Under increasing axial tension the torsional stress-strain behaviour displays an increasing hysteresis.
    a. The torsional dampening, expressed as energy loss per loading/unloading cycle. ranges from XX% to xx%. This is much higher than the typical internal torsional damping in steel drill pipe.
    b. The typical external torsional dampening caused by fluid drag and borehole friction while drilling is in the order of 50%. The effect of internal damping caused by hysteresis during torsional loading of GRE casing is therefore noticeable, and results in a further beneficial decrease in the critical rotary speed for stick-slip torsional vibrations.

7.2 Recommendations

1. Equip the push beam of the test bench with sliders so it won't grip into the U-beams.
2. Use a laser system which can be hooked up to a data logger to measure the elongation.
3. Design a different measuring system tangentially so it can measure larger increases in angular displacement time wise
    a. Increase the dynamic loading to frequencies that correspond to the natural frequency of the drill string.

Appendices

Appendix A Exact layering of the GRE pipe

The table below shows the type of layering its weight, volume fraction, its thickness and the direction of the fibres in that layer. The ± sign tells you that this layer has those two directions.

	Fiber layer type	Layer weight gr/m2	Fiber Volume factor	Position to X axle (longitudinal)	Layer thickness mm
1	**Random layer**	450	0.200		0.9
2	**Cross layer**	800	0.500	±77	0.64
3	**Cross layer**	800	0.500	±45	0.64
4	**Cross layer**	800	0.500	±77	0.64
5	**Unidirectional mat**	800	0.420	17	0.76
6	**Cross layer**	800	0.500	±45	0.64
7	**Cross layer**	800	0.500	±77	0.64
8	**Cross layer**	800	0.500	±45	0.64
9	**Unidirectional mat**	800	0.420	17	0.76
10	**Cross layer**	800	0.500	±45	0.64
11	**Unidirectional mat**	800	0.420	17	0.76
12	**Cross layer**	800	0.500	±45	0.64
13	**Unidirectional mat**	800	0.420	17	0.76
14	**Cross layer**	800	0.500	±45	0.64
15	**Cross layer**	800	0.500	±77	0.64
16	**Cross layer**	800	0.500	±45	0.64
17	**Unidirectional mat**	800	0.420	17	0.76
18	**Cross layer**	800	0.500	±77	0.64
19	**Cross layer**	800	0.500	±45	0.64
20	**Cross layer**	800	0.500	±77	0.64
21	**Random layer**	450	0.200		0.9

Table 1: This table gives the build up of the pipe. It shows the type of layer, its weight, volume fraction, its thickness and the direction of the fibres in that layer.

GRE	**Fiber type**	**Resin**	**Epoxy cure**		
	E-glass	Epikote 827	Epikure 960		
Steel	**Type**				
	E-470				

Table 2: Here you can find the specification off the materials used in the casing pipe.

Appendix B Matlab code torsional vibrations

```
% Script file to simulate torsional vibrations in a GRE drill string

clear all
close all

% Conversion factors:
inch    = 2.54;                 % [inch]
% Input data:
D_c_o   = 9;                    % [inch] collar outer diameter
D_c_o   = D_c_o*inch*0.01;      % [m] collar outer diameter
D_c_i   = 3;                    % [inch] collar inner diameter
D_c_i   = D_c_i*inch*0.01;      % [m] collar inner diameter
D_dp_o  = 5;                    % [inch] drill pipe outer diameter
D_dp_o  = D_dp_o*inch*0.01;     % [m] drill pipe outer diameter
D_dp_i  = 4.3;                  % [inch] drill pipe inner diameter
D_dp_i  = D_dp_i*inch*0.01;     % [m] drill pipe inner diameter
BIT_od  = 6                     % [inch] bit OD
L_c     = 150;                  % [kg] weight of drill pipe per segment
L_p     = 10;                   % [m] length of pipe sections
L_dp    = 2000;                 % [m] length of drill string
G       = 8.35*10^9;            % [N/m^2] shear modulus GRE = 8.35*10^9;
t_start = 0;                    % [s] initial time
t_end   = 100;                  % [s] end time
c       = 0.063;                % [Ns/rad] damping coefficient per unit length
epsilon = 10e-3;                % [rad/s] value near to zero to simulate standstill drill bit
Omega   = 40*pi/30;             % [rad/s] rotational velocity initial rotation
T_sl    = 2000;                 % [Nm] slipping torque on bit
T_st    = 4000;                 % [Nm] sticking torque on bit

% Intermediate data:
V_dp       = pi*L_p*((D_dp_o/2)^2-(D_dp_i/2)^2); % [m^3] volume of drill pipe
I_c        = pi/32*(D_c_o^4-D_c_i^4);            % [m^4] collar polar moment of inertia
I_dp       = pi/32*(D_dp_o^4-D_dp_i^4);          % [m^4] drill pipe polar moment of inertia
J_tilde_c  = rho_c*I_c;                          % [kg m^2] collar mass moment of inertia per
unit length
J_tilde_dp = rho_dp*I_dp;                        % [kg m^2] drill pipe mass moment of inertia per
unit length
J          = L_c*J_tilde_c + (L_dp*J_tilde_dp)/3;  % [kg m^2] rotational inertia
k          = G*I_dp/L_dp;                        % [Nm/rad] equivalent torsional stiffness
c1         = L_dp*c/3;                           % [Nms/rad] equivalent damping coefficient
```

Appendix C The well trajectory of the input data and an extension on the equations used for the TanD calculations

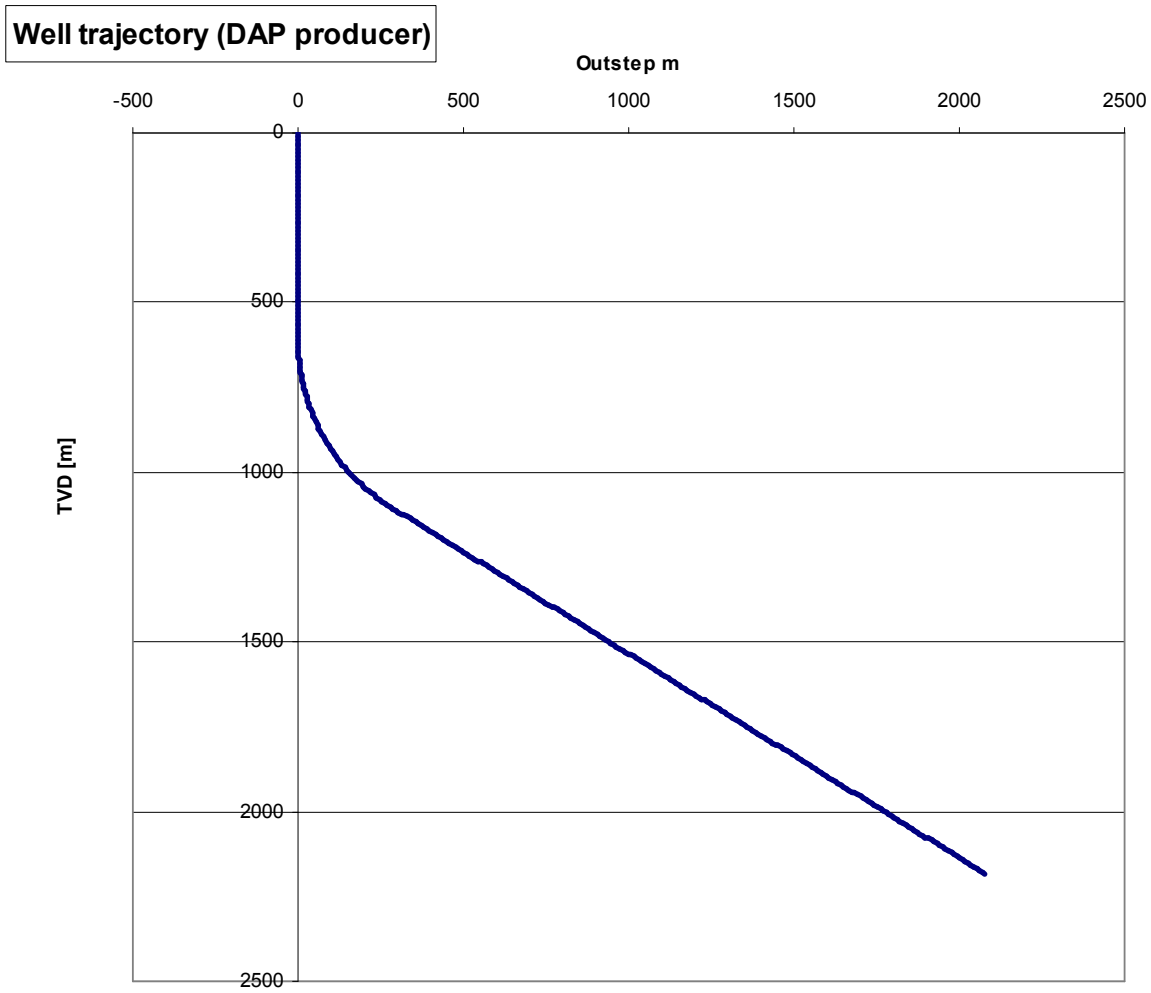


Fig 1: Well plan of the producer.

Data input			
Descr	**Symbol**	**value**	**value**
Comp. s.g.	**sgst**	2,6	**kg/ltr**
Dir Azimuth	**azi**	180	**deg**
Pipe ID	**PID**	6,11	**in**
Pipe OD	**POD**	7,265	**in**
OD coupling	**PODC**	8,125	**in**
Mudweight	**rho**	1,32	**kg/ltr**
Csg depth	**CD**	700	**m**
Mod of el	**E**	3,00E+06	**psi**
Mod of el	**G**	2,00E+06	**psi**
Lat contr	**v**	0,33	**[-]**
AH depth	**AHD**	3300	**m**
Correction		1	

Table 3: Input data used to calculate the TanD of the producer.

Torque and drag equations

F_i, where $i = 10m$ is the cell in the spreadsheet, will be calculated simply by calculating the weight of that 10m section of the drill pipe as follows

$$F = w * \sin(I)$$

Where w is the weight of the drill pipe per meter. I is the vertical inclination in radians. When the well is inclined less force is in the vertical direction thus simulating the section lying on the borehole.

The drag created by the drill string when pulling out is calculated as follows.

$$D_i = \mu \times \left(F_{i+1} \times n_i^v - P_i \right) + F_{i+1} \times n_i^h$$

n_i^v & n_i^h are the resultant vector factors of the force in due to dog leg severity in vertical and horizontal direction respectively. Here μ is the friction factor P_i is the resultant vector of the weight in of the section in the vertical direction due to the weight of the section.

The torsion is calculated according to the next equation:
$T_i = \mu \times \left(R_{i+1} \times n_i^v - P_i \right) + R_{i+1} \times n_i^h) \times c / 2$ where R_i is the rotating weight.

References

Bert, C.W.: *Composite Materials: a Survey of the Damping Capacity of Fibre Reinforced Composites,* Damping Applications for Vibrations Control., 1980 53-63

Gdoutos, E.E., Daniel, I.M.: *Non linear Stress and Deformation Behaviour of Composite Sandwich Beams*, Applied Mechanics and Materials, 2008, 13-14, 91-98.

Gibson, R.F., Plunkett, R.: *Dynamic Stiffness and Damping of Fibre Reinforced Composite Materials*, The Shock and Vibration Digest, 1979, 11, 53-63.

Hahn, H.T., Tsai, W.: *Nonlinear Elastic Behaviour of Unidirectional Composite Laminae,* Journal of Composite Materials, 1973, 7, 102-118.

Hopkins, B.F.R.S, Williams, G.T.: *The elastic hysteresis of steel,* Proceedings of the Royal Society of London. Series A, Containing Papers of a Mathematical and Physical Character, 1912, Vol. 87, No, 598, pp. 502-511

Jansen, J.D. 1993: *Nonlinear Dynamics of Oilwell Drillstrings*. Delft: Delft University Press.

Johancsik, C.A. Friesen, D.B. Dawson, R. Torque and Drag in Directional Wells-Prediction and Measurement

Knox E.M., Lafferty S., Cowling M.J., Hashim S.A.: *Design guidance and structural integrity of bonded connections in GRE pipes*, Composites Part A: Applied manufacturing and sciences*,* 2001, **32** 231-241

Kocks, UF. Stout, M.G. 1999 *Torsion testing for general constitutive relations: Gilles Canova's Master's Thesis*

Leslie J.C., Jean J,R., Neubert H., Truong .: *Development and Manufacture of Cost Effective Composite Drill Pipe.* 2000

Mitchel, R.F., Samuel, R. 2009. How good is the torque/drag model. Paper SPE 105068, *Drilling & Completion.*

Ogihara, S., Reifsnider, K.L.: *Characterization of Behaviour in Woven Composite Laminates,* Applied Composite Materials., 2002, 9, 249-263

Singh, S.P., Gupta, K.: *Damped Free Vibration of Layered Composite Cylindrical Shells,* Journal of Sound and Vibration., 1994, 172(2), 191-209.

Tucker R.W., Wang C., *An Integrated Model for Drill-String Dynamics.* Department of Physics, Lancaster University, LA1 4YB, England, 1999

Yoshihara, H. Ohta, M. Origuchi, K. 1998 *Formulation of Shear Stress/Shear Strain Relationship Using the Torsion Testing Data*. Bulletin Tokyo University.